Polymer Reinforced Solder Paste for Improving Impact Energy Absorption Capability in Micro LED Laser-Assisted Mass Transfer

Ji, Liangzheng; Li, Zaihuan ; Zhang, Guoqi; Zhang, Jing ; Liu, Pan

DOI
10.1109/SSLChinaIFWS60785.2023.10399660

Publication date
2023

Document Version
Final published version

Published in
Proceedings of the 2023 20th China International Forum on Solid State Lighting & 2023 9th International Forum on Wide Bandgap Semiconductors (SSLCHINA: IFWS)

Citation (APA)
Ji, L., Li, Z., Zhang, G., Zhang, J., & Liu, P. (2023). Polymer Reinforced Solder Paste for Improving Impact Energy Absorption Capability in Micro LED Laser-Assisted Mass Transfer. In *Proceedings of the 2023 20th China International Forum on Solid State Lighting & 2023 9th International Forum on Wide Bandgap Semiconductors (SSLCHINA: IFWS)* (pp. 365-368). IEEE. https://doi.org/10.1109/SSLChinaIFWS60785.2023.10399660

2023 20th China International Forum on Solid State Lighting & 2023 9th International Forum on Wide Bandgap Semiconductors (SSLCHINA: IFWS) | 979-8-3503-8537-3/23/$31.00 ©2023 IEEE | DOI: 10.1109/SSLCHINAIFWS60785.2023.10399660

Polymer Reinforced Solder Paste for Improving Impact Energy Absorption Capability in Micro LED Laser-assisted Mass Transfer

Liangzheng Ji[1, 2], Zaihuan Li[2], Xin Wang[2], Guoqi Zhang[3], Jing Zhang[2], and Pan Liu[1 *]
[1] Faculty of Academy for Engineering and Technology, Fudan University
Shanghai, China
[2] Heraeus Material Technology Shanghai Ltd.
Shanghai, China
[3] Electronic Components, Technology, and Materials, Delft University of Technology
Delft, Netherlands
panliu@fudan.edu.cn

Abstract

Micro LED displays offer superior performance compared to traditional LCD and OLED displays. However, challenges in transfer technology, such as high throughput and scalability, must be addressed. Among various mass transfer techniques, stamp transfer and laser-assisted transfer are widely used for Micro LED assembly. The laser-assisted transfer technique enables high-speed and accurate transfer. Anisotropic conductive film (ACF) is commonly used for its energy absorption properties during chip transfer. However, during the subsequent thermocompression bonding process, the ACF film needs to be ruptured, which adds no value to the bonding process. To address limitations, we have developed a polymer-reinforced solder paste that demonstrates high effectiveness in absorbing impact energy during chip dropping, providing performance comparable to ACF-like materials for die receiving. It also possesses typical solder paste characteristics, enabling the formation of reliable solder joints between the chip and substrate. This material facilitates streamlined manufacturing process and providing opportunities for chip rework in subsequent stages.

Introduction

The increasing demand for high-performance displays across extensive applications, in smart devices and technologies, such as smartwatch, smartphone, wearable devices, outdoor displays, naked eye 3D, and virtual reality/augmented reality, drives the need for high-resolution, transparent, and flexible display technologies in the future.[1-3] Micro-LED displays, characterized by extended lifetime, short response time, low power consumption, and high brightness, have the potential to replace traditional liquid crystal displays (LCDs) and organic light-emitting diode (OLED) technologies. However, to ensure a prominent position in the future display landscape, micro-LEDs must address challenges associated with mass transfer and high manufacturing costs. The fabrication of high-resolution micro-LED displays presents complex difficulties due to the precise assembly of millions of micro-sized light-emitting diodes onto driving circuits. [1, 2, 4]

Numerous mass transfer methods have been developed in the field of Micro LED technology, including electrostatic transfer, magnetic force transfer, elastomer stamp transfer, fluidic self-assembly, laser-assisted transfer, and roll printing. [1, 5-9] Stamp transfer and laser-assisted transfer have emerged as the most widely adopted techniques for Micro LED mass transfer. Laser technology has been extensively utilized in various Micro LED processing steps, such as dicing, surface texturing, annealing, mass transfer, laser lift-off (LLO), and defect reworking. [10-12] The laser-assisted mass transfer process in Micro LED technology involves laser irradiation inducing thermal decomposition of gallium nitride (GaN) or causing a phase change in the dynamic release layer (DRL). [10-13] This creates a gas that propels Micro LEDs towards the receiver substrate. Notably, the laser-assisted transfer technique has garnered substantial interest due to its distinct advantages, including high transfer speed, yield, accuracy, selectivity, and the capability for noncontact interactions. In this process, the sacrificial layer undergoes decomposition, leading to the evolution of gas. Consequently, the chip undergoes a rapid descent, deviating from the conventional die picking and placing process known for its slower or negligible drop speed. However, this accelerated drop of the die necessitates the presence of a receiving material capable of efficiently absorbing the high-impact energy.

Anisotropic conductive film (ACF), consisting of a non-conductive film and conductive metal particles, is extensively used in Micro LED assembly due to the elasticity of the film, which enables the effective absorption of high-impact energy during the transfer process. [14-15] These particles facilitate electrical connectivity when compressed between the Micro LED die bumping and backplane pads. ACF offers advantages such as smaller bonding pitches, however, its practicality is limited by the size and cost of the conductive particles, rendering it less suitable for bonding with pitches smaller than 10 μm. Nonetheless, ACF exhibits certain drawbacks including increased contact resistance, lower thermal conductivity, and reduced adhesion and moisture reliability. Furthermore, during the subsequent thermocompression bonding process, the ACF film needs to be ruptured, which does not provide any advantages or value to the bonding process. [15]

In this study, we have successfully developed a novel material known as polymer-reinforced solder paste. The polymer reinforced solder paste exhibits exceptional efficiency in absorbing impact energy during chip dropping, demonstrating performance comparable to ACF-like materials for die receiving. The unique structure of the polymer reinforced system, as depicted in the Fig.1, schematic diagram, allows for the absorption or dissipation of energy through mechanisms such as breaking of hydrogen bonding, stretching of polymer chains, and entanglement. A rapid characterization technique, nominated as the pressing method, to evaluate the compressive resistance of materials. This

979-8-3503-8537-3/23/$31.00 ©2023 IEEE

method quantifies the change in height of various materials when subjected to a fixed momentum, enabling the assessment of their energy absorption capability. In our internal simulation experiment, we observed that the buffering capacity of the polymer-reinforced solder paste was almost twice as high as the compared solder paste. This enhanced buffering capacity yielded a significantly improved die receiving effect in the practical laser-assisted mass transfer process. Additionally, the material demonstrates typical characteristics of solder paste, enabling the formation of reliable solder joints between the chip and substrate. By implementing this approach, the limitations imposed by ACF in laser-induced mass transfer can be effectively addressed. This breakthrough in material design streamlines the manufacturing process and provides potential opportunities for chip rework in subsequent stages, enhancing overall efficiency and productivity.

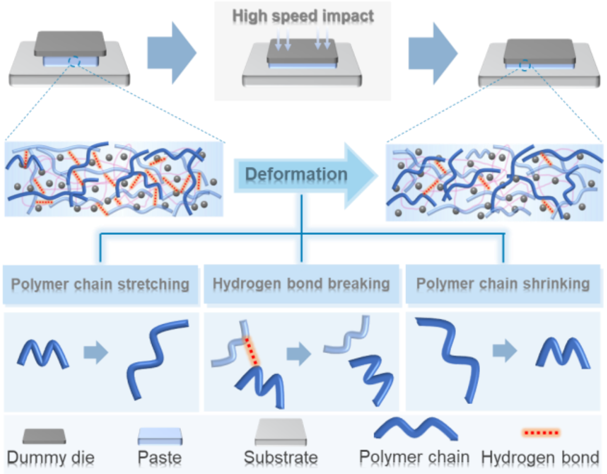

Fig.1. Schematic diagram of polymer-reinforced paste buffering high speed impact energy.

Experimental

The experimental methodology, as depicted in the schematic diagram (Fig. 2), involves several steps including paste printing, die placement, pressing, and the measurement of the height from the die top to the substrate surface. Starting with the paste printing process, the paste is placeed on the stencil surface, the stencil has specific characteristics: a thickness of 100 µm and a square opening with a side length of 5mm. Printing of the paste onto the stencil is performed under a pressure of 18 N and at a speed of 20mm/s. After printing, a dummy die is gently placed on the paste.

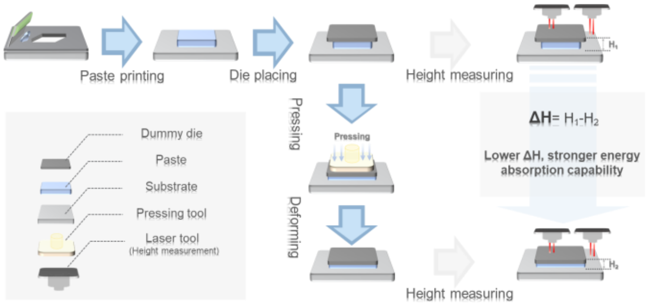

Fig.2. Schematic diagram of the pressing method testing process.

Subsequent measurement of the height from the top of the die to the substrate surface is performed using a laser tool. The obtained height (H_1) is then recorded. Following this, the die is pressed using a tool imparting a specific momentum, inducing deformation in the paste. After removing the pressing tool, the height measurement is repeated, and the result (H_2) is recorded. The difference in height, denoted as ΔH (H_1-H_2), represents the deformation of the paste; lower ΔH values are indicative of smaller deformations and stronger energy buffering capabilities. On the contrary, higher ΔH values suggest weaker energy buffering capabilities.

Results and discussions

In this study, the “pressing” method was utilized, and commercialized solder paste from Heraeus was employed to investigate the optimal parameters for distinguishing variations among candidates. Fig. 3 illustrates the examination of different momenta (0.5 N·s, 1 N·s, 1.5 N·s, 2 N·s, 4 N·s, 6 N·s, 8 N·s, and 12 N·s) and the resulting changes in ΔH (initial height variation).

Initially, as the momentum increased from 0.5 N·s to 2 N·s, ΔH exhibited a significant rise from 1.1 µm to 51.3 µm. Subsequently, further momentum increases from 2 N·s to 12 N·s led to a marginal ΔH increase from 51.3 µm to 59.3 µm, indicating stabilization within a certain range. Considering that the original height after placing the dummy die and prior to pressing was approximately 70 µm, the size distribution of particles in the paste ranged from 5 µm to 15 µm. Consequently, in this specific application, material deformation occurred notably with small momentum implementation. However, as the momentum reached a specific threshold, most of the deformation was completed, and the solder particles provided structural support, resulting in negligible ΔH changes. Based on these findings, a momentum value of 1.5 N·s was selected as the optimal parameter for the subsequent formulation study to ascertain its effectiveness and determine the viability of other candidates.

To explore the effect of the polymer on the energy absorption capability during compression, a proprietary polymer material was introduced in this study. Different concentrations of the polymer (1%, 2%, and 3%) were added to the standard paste, resulting in the formation of various polymer-reinforced solder paste formulations. The standard paste was also included as a comparison reference to assess the influence of the polymer. In the experimental setup, a momentum of 1.5 N·s was implemented.

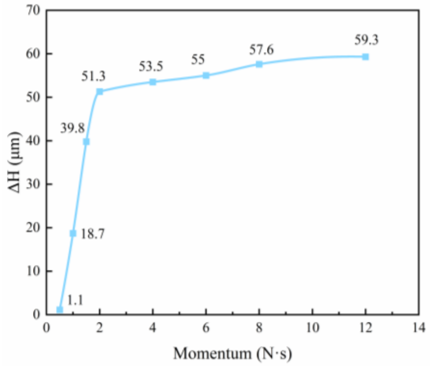

Fig.3. The variation of ΔH (height difference) in response to momentum changes of the commercial paste.

979-8-3503-8537-3/23/$31.00 ©2023 IEEE

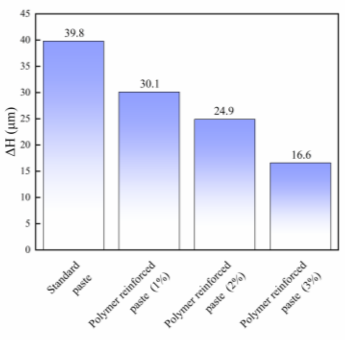

Fig.4. The comparison among standard solder paste and polymer reinforced solder paste with different concentrations.

The findings depicted in Fig. 4 reveal distinct and noteworthy trends. With the incorporation of 1% polymer, a significant decrease in ΔH was observed, recording a notable shift from 39.8 μm to 30.1 μm. This reduction indicates the advantageous impact of the polymer in enhancing energy absorption capability. Furthermore, as the polymer concentration increased from 1% to 2% and subsequently to 3%, a gradual decline in ΔH was consistently observed, reaching values of 24.9 μm and 16.6 μm, respectively. These results provide robust evidence supporting the notion that polymer reinforcement contributes towards fortifying the inner structure, resulting in improved compression resistance.

The viscosity of the solder paste increases proportionally with higher polymer concentration. From a fundamental mechanism perspective, higher viscosity implies a stronger compression resistance capability, as it signifies a more robust internal structure capable of withstanding external forces. Therefore, to ensure consistent viscosity levels, we implemented three different methods to control paste viscosity. Specifically, slight adjustments were made to the proprietary polymer, polyamide, and rosin additives concentration in the formulation, respectively. At here, we selected the polymer-reinforced solder paste with 3% polymer content. For the polyamide and rosin modified solder pastes, the amount of adjustment depended on the viscosity comparison with the polymer-reinforced paste. As depicted in Fig. 5, the polymer-reinforced solder paste exhibited a viscosity of 255 Pa·s with a corresponding ΔH value of 16.6 μm. The polyamide-modified solder paste exhibited a viscosity of 258 Pa·s with a ΔH value of 18.5 μm, while the rosin-modified solder paste exhibited a viscosity of 244 Pa·s with a ΔH value of 21.2 μm. From an energy absorption perspective, as indicated by ΔH, the polymer-reinforced paste exhibited slightly better performance than the polyamide-modified paste and significantly outperformed the rosin-modified paste. However, it is worth noting that excessive use of polyamide and rosin additives resulted in unexpected issues, such as paste drying and excessive stickiness that affected the paste release during application. These phenomena had a significant impact on paste application. In contrast, the proprietary polymer not only exhibited superior energy resistance capability but also had no adverse effects on practical application.

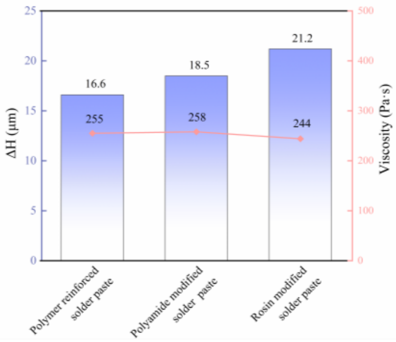

Fig.5. The comparison among polymer reinforced solder paste, polyamide modified solder paste, and rosin modified solder paste.

Based on the findings, the polymer-reinforced solder paste containing 3% polymer content exhibited promising potential in terms of compression resistance capability. Subsequently, we applied this paste in the actual laser mass transfer process and compared its performance with commercial solder paste. During this process, the dies were placed on the backside of the dynamic release layer (DRL), and upon laser beam exposure, the dies dropped rapidly, impacting the surface of the solder paste that was printed onto the substrate using stencil printing. Concerning the standard solder paste, we observed that most of the dies were missed, either bouncing off the surface or merging into the material, leaving small marks behind. Although a few dies landed successfully, there were considerable issues with die placement. In contrast, when using the newly designed polymer-reinforced solder paste, all the dies landed well on the target area, with no bouncing or missing dies. However, some angular deviations and slight shifting issues were observed. Overall, the polymer-reinforced solder paste demonstrated superior performance compared to the non-reinforced counterpart, although further improvements are still necessary. the die receiving performance of the polymer-reinforced solder paste closely aligns with that of the anisotropic conductive film (ACF) in this application. These outcomes provide supporting evidence for the feasibility of the proposed polymer-reinforced structure and validate the efficacy of the designed pressing simulation method in differentiating variations among different solder pastes.

Building upon the achievements derived from our custom-designed paste, we conducted a comprehensive solderability study using our internal test vehicle. This entailed a series of steps including paste printing, 4*6 mil² LED die picking and placing, followed by reflowing in a nitrogen-protected oven where the oxygen concentration was maintained below 100 ppm. The process culminated with a thorough performance inspection. Fig. 6(a) and (b) present X-ray images showcasing the solder joint formation of the standard solder paste and the polymer-reinforced solder paste. Both pastes produced robust solder joint formations as observed in the thicker metal layer indicated by the dark black areas. These areas essentially signify the solder joint formation between the die and the substrate's pad. To further evaluate the void performance for the solder joints, we employed a high-resolution X-ray machine. As depicted in Fig. 7, the void distribution of the solder joints for both the polymer-reinforced and standard solder pastes displayed similar trends. For the standard solder paste, most of the voiding under the dies was calculated to be 0%, with some joints exhibiting voiding ranging from 1% to

7%. Interestingly, the voiding distribution for the polymer-reinforced paste aligned with the standard paste, with most voids registering at 0% and some ranging from 1% to 5.5%. Generally, the acceptable specification for solder voiding is within 10%, and both pastes adhered to this specification. These findings sufficiently demonstrate that the polymer solder paste does not compromise the solderability performance whilst offering high potential for absorbing impact energy.

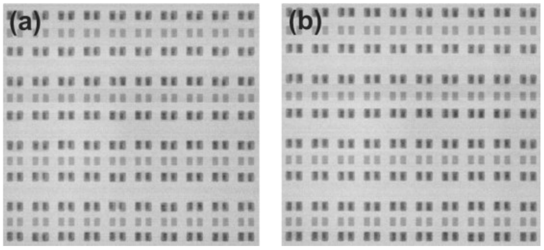

Fig. 6. The X-ray images of (a) standard solder paste and (b) polymer reinforced solder paste.

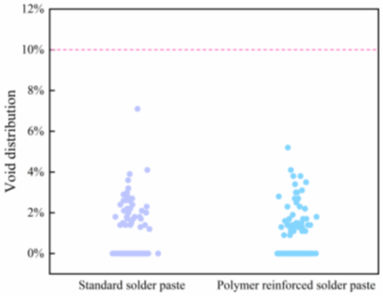

Fig. 7. The void distribution of standard and polymer reinforced solder paste.

Conclusions

In conclusion, this study has successfully developed a novel material, the polymer-reinforced solder paste, which demonstrates remarkable compression resistance capabilities. Simultaneously, we have established a corresponding evaluation method, termed ‘Pressing’, that can be utilized to validate the differences among various formulations. This method leverages the ΔH index to gauge material variation. Through this method, we observed that the optimal polymer-reinforced solder paste formulation resulted in an almost 60% improvement in ΔH compared to the commercial standard paste. Furthermore, the newly developed paste showed outstanding efficiency in absorbing impact energy during laser-assisted transfer, with its performance being comparable to that of ACF-like materials for die receiving. This innovation has retained exceptional soldering performance without any displayed compromise in utility. Future research endeavors can delve into a comprehensive investigation of the underlying mechanisms through which the polymer-reinforced solder paste enhances energy buffer capability. This exploration will contribute to a deeper understanding and facilitate the development of similar materials. Consequently, it will propel the commercialization of Micro LED display technology, ultimately bringing this cutting-edge technology into the hands of the general public.

Acknowledgments

The authors would like to thank the Heraeus-Fudan University cooperation project.

References

1. Zhou, X., et al. "Growth, transfer printing and colour conversion techniques towards full-colour micro-LED display." Progress in Quantum Electronics Vol. 71 (2020): 100263.
2. Ding, K., et al. "Micro-LEDs, a manufacturability perspective." Applied Sciences Vol. 9, No. 6 (2019): 1206.
3. Anwar, A. R., et al. "Recent progress in micro-LED-based display technologies." Laser & Photonics Reviews Vol. 16, No. 6 (2022): 2100427.
4. Ji, L., et al. "An Alternative Micro LED Mass Transfer Technology: Self-Assembly." 2022 23rd International Conference on Electronic Packaging Technology (ICEPT). IEEE, 2022.
5. Chang, W., et al. "Concurrent self-assembly of RGB microLEDs for next-generation displays." Nature (2023): 1-5.
6. Whitesides, G. M., et al. "Self-assembly at all scales." Science Vol.295, No. 5564 (2002): 2418-2421.
7. Meitl, M. A., et al. "Transfer printing by kinetic control of adhesion to an elastomeric stamp." Nature materials Vol.5, No. 1 (2006): 33-38.
8. Pan, Z., et al. "Wafer-scale micro-LEDs transferred onto an adhesive film for planar and flexible displays." Advanced Materials Technologies Vol. 5, No. 12 (2020): 2000549.
9. Kim, R.-H., et al. "Stretchable, transparent graphene interconnects for arrays of microscale inorganic light emitting diodes on rubber substrates." Nano letters Vol. 11, No. 9 (2011): 3881-3886.
10. Gong, Z., et al. "Layer-scale and chip-scale transfer techniques for functional devices and systems: a review." Nanomaterials Vol. 11, No. 4 (2021): 842.
11. Gong, Y., et al. "Laser-Based Micro/Nano-Processing Techniques for Microscale LEDs and Full-Color Displays." Advanced Materials Technologies Vol. 8, No. 5 (2023): 2200949.
12. Mikulics, M., et al. "Conditioning nano-LEDs in arrays by laser-micro-annealing: The key to their performance improvement." Applied physics letters Vol. 118, No. 4 (2021).
13. Marinov, V. R., et al. "52-4: Laser-Enabled Extremely-High Rate Technology for μLED Assembly." SID Symposium Digest of Technical Papers. Vol. 49. No. 1. 2018.
14. Mun, S.-H., et al. "Highly Efficient Full-Color Inorganic LEDs on a Single Wafer by Using Multiple Adhesive Bonding." Advanced Materials Interfaces Vol. 8, No. 14 (2021): 2100300.
15. Choi, K.-S., et al. "Simultaneous transfer and bonding (SITRAB) process for Micro-LEDs using laser-assisted bonding with compression (LABC) process and SITRAB adhesive." 2021 IEEE 71st Electronic Components and Technology Conference (ECTC). IEEE, 2021.